Finite Element EEG and MEG Simulations for Realistic Head Models: Quadratic vs. Linear Approximations

Van Uitert R[1], Weinstein D[1], Johnson C[1], and Zhukov L[2]

[1]University of Utah, Salt Lake City, USA
[2]California Institute of Technology, Pasadena, USA

Introduction

Many researchers use homogeneous, isotropic concentric sphere models when simulating the electric potentials from neuronal activity in the brain as measured by electroencephalography (EEG), and the resulting external magnetic fields as measured by magnetoencephalography (MEG). The corresponding source model usually assumes that neurons act as current electric dipoles [2] such that the EEG and MEG forward problems can be reduced to closed form analytic solutions. With more realistic, inhomogeneous, anisotropic, non-spherical head models, however, a closed form solution is not as easily computed and approximations, such as finite element methods, must be used.

The simplest numeric finite element method employs linear basis functions to approximate the physical equations governing the electric and magnetic fields $[2, 4, 7]$ and uses a constant electric gradient within an element. In contrast, a closer approximation of the physical equations and a non-constant electric gradient within an element $[1, 3, 9]$ may be made by using a higher order finite element method. As an initial part of understanding the accuracy and computational effects of using higher order basis functions, we used both linear and quadratic finite element methods to calculate the electric and magnetic fields detected by EEG and MEG, respectively, and compared the results.

Method

For a current dipole within a conductive region, G, of the brain with conductivity σ and homogeneous magnetic permeability μ_0 the quasistatic approximations of Maxwell's equations, Poisson's equation, and the Biot-Savart law can be used to determine the electric field, E, and the magnetic field, B, as follows:

$$E = -\nabla\phi \quad (1)$$

$$-\nabla\cdot(\sigma(r)\nabla\phi(r)) = \nabla I(r) \quad (2)$$

$$B(r) = \mu_0/4\pi[Q\times(r-r')/|r-r'|^3 - \int_{G_j}\sigma_j(r)\nabla\phi\times(r-r')/|r-r'|^3 dv'] \quad (3)$$

where ϕ is the electric potential, I is the electric current, r' is the coordinate of the dipole, r is the point of detection, and Q is the dipole moment.

If the conductor enclosing a dipole is a homogeneous sphere, the electric potential [10] can be calculated from an analytic closed form equation as follows:

$$\begin{aligned}\phi(r) &= Q/4\pi\sigma\cdot[(r-r')/r_p^3 + (r-|r|^2r'/R^2)/R^3r_{pi}^3 \\ &\quad +1/R^3r_{pi}[r+(r|r'||r|/R^2cos\theta \\ &\quad -|r|^2r'/R^2)/r_{pi} + 1 - |r'||r|cos\theta/R^2]] \quad (4)\end{aligned}$$

where $r_p = (|r|^2+|r'|^2-2|r||r'|cos\theta)^{1/2}$, $r_{pi} = (1 + (|r||r'|/R^2)^2 - 2|r'||r|cos\theta/R^2)^{1/2}$, θ is the angle between r and r', and R is the radius of the sphere.

Further, according to Sarvas [8], the magnetic field outside of a homogeneous sphere enclosing a dipole can be calculated as follows:

$$B(r) = \mu_0/4\pi F^2(FQ\times r' - Q\times r'\cdot r\nabla F) \quad (5)$$

where $F = |a|(|r||a| + |r|^2 - r'\cdot r)$, $a = r - r'$, and $\nabla F = (|a|^2/|r| + a\cdot r/|a| + 2|a| + 2|r|)r - (|a| + 2|r| + a\cdot r/|a|)r'$.

In our simulations, the finite element method was used to calculate electric and magnetic fields in discrete, numeric models of both spheres and realistic heads. The SCIRun and BioPSE problem solving environments [5] were used to drive the forward EEG and MEG simulations.

Results

Several tests were used to compare the accuracy of the linear versus the quadratic finite element methods. Using a sphere, we calculated the electric potentials and magnetic field by our numeric model and compared it to the analytic electric potential (4) and magnetic field (5) equations, respectively. The sphere tests were performed on five different unit decimeter spheres containing the following number of elements: 41,093, 112,547, 222,928, 347,647, and 459,784. A dipole was placed in the sphere at (0.8,0.5,0) with moment (1,-0.5,0).

For each sphere, electric fields were numerically calculated using both linear and, separately, quadratic finite element methods and compared to the analytic solution. The relative root-mean-square (RMS) percentage error for the electric numeric solution compared to analytic electric potential values is shown in Figure 1 for both the linear and quadratic models. Also for each sphere, the magnetic fields were numerically calculated using both the linear and, separately, the quadratic finite element methods and compared to the analytic solution. The relative RMS percentage error for the magnetic numeric solution compared to analytic values is shown in Figure 2 for both the linear and quadratic models. The wall-clock runtimes for the above electric and magnetic numeric calculations for both the linear and quadratic methods appear in Table 1.

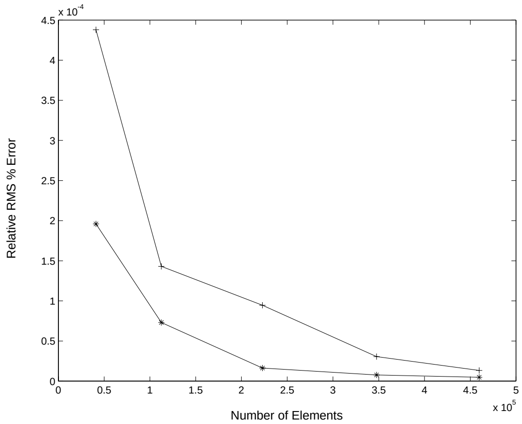

Figure 1: Error of electric potential calculations versus number of elements in spherical mesh (crosses indicate linear solution and stars indicate quadratic solution).

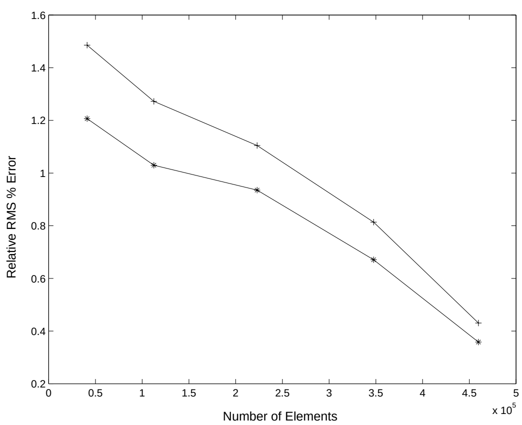

Figure 2: Error of magnetic field calculations versus number of elements in spherical mesh (crosses indicate linear solution and stars indicate quadratic solution).

The next comparison performed was the accuracy of the linear versus quadratic methods for various distances between the dipole and detectors. Using the unit sphere containing 222,928 elements, the dipole was placed at positions 0.03, 0.13, 0.31, 0.48, and 0.83 decimeters from the electrode and magnetic detector positions. Figure 3 illustrates the relative RMS percentage error differences between the linearly and quadratically calculated electric potentials at the different dipole positions in the unit sphere. Figure 3 also contains the relative RMS percentage error differences between the linearly and quadratically calculated magnetic values at the different dipole positions in the unit sphere.

Finally, the linear and quadratic numeric finite ele-

Table 1: Runtimes (in seconds) of linear versus quadratic, electric and magnetic calulations.

Num Elements	*Electric*		*Magnetic*	
	Linear	*Quad*	*Linear*	*Quad*
41093	3	35	14	58
112547	6	127	42	192
222928	15	220	93	362
347647	22	351	151	572
459784	30	467	210	760

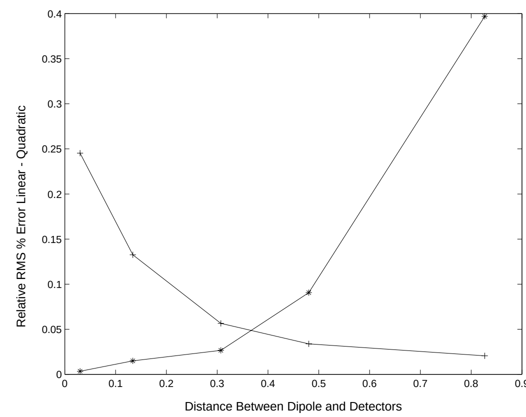

Figure 3: Difference between calculated linear and quadratic error of electric potentials (crosses) and magnetic values (stars) versus distance between dipole and detectors.

ment methods for EEG and MEG forward simulations were performed on a realistic head model consisting of 396,285 elements and 64 detectors placed over the head. This model was constructed from a volume MRI scan and consisted of six conductivity values [6]. A tangentially-oriented dipole was placed in the right parietal lobe. The relative RMS percentage difference between the linearly and quadratically calculated electric potentials at the electrodes was 2.78%. The relative RMS percentage difference between the linearly and quadratically calculated values at the magnetic detectors was 15.75%. Figure 4 permits a visual comparison between the accuracy of the linear and quadratic finite element methods in calculating the electric potentials on the brain cortex.

Discussion

The tests performed with the spherical models and the comparison of the results with those obtained using the analytic solutions show that our model using the quadratic finite element method works accurately. Further, Figures 1 and 2 demonstrate that for all five spheres, the quadratic method consistently results in less error than does the linear method. The difference in errors between the electric potentials calculated by the linear and quadratic methods, however, decreases as the number of elements progresses from 41,093 to 459,784 elements. This decrease results from the $1/r^2$ component of the dipole's physical equations; these equations can be better represented by a quadratic finite element

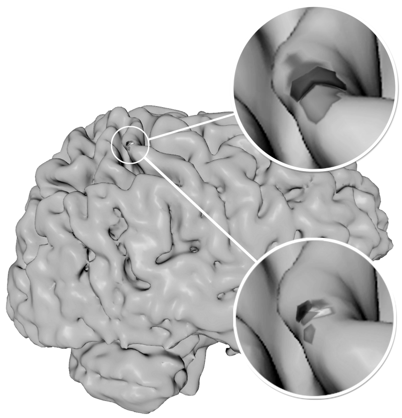

Figure 4: Electric potential on brain cortex calculated using the linear finite element method (in the upper panel) and the quadratic finite element method (in the lower panel).

model than a linear model when elements are very large, but as elements become smaller the linear basis functions can more accurately approximate the quadratic equations. The difference between linear and quadratic methods of calculating magnetic values also decreases with increasing number of elements, but in a more linear fasion.

Figure 3 shows that the error in electric potentials calculated by the linear method relative to the quadratic method increases greatly as the detector positions approaches the dipole, reflecting the $1/r^2$ fall-off of the dipole's field strength with distance and the higher gradient of the electric field lines near the dipole than at farther distances. The magnetic field due to the dipole's volume currents, which is modeled by the integral portion of Equation 3, is derived from the electric potentials throughout the conductive medium, whereas the remainder of the equation models the magnetic field due to the dipole's primary current [4]. The magnetic field due to volume currents increasingly dominates the magnetic field due to the primary current as the distance between the dipole and detectors increases; since the magnetic values due to volume currents are derived from electric potentials which are better approximated by the quadratic than the linear method, the error in the magnetic values calculated by the linear method increases greatly compared to the values calculated by the quadratic method as the magnetic field detector moves away from the dipole.

The advantages of the increased accuracy of the quadratic method, as demonstrated in spherical models, becomes even more useful in the realistic head model. Figure 4 shows that the quadratic element method calculates the electric potential to a more focussed region than does the linear element method; the quadratic method can determine dipole positions within a particular element, whereas the linear method cannot.

The error in the electric potentials and magnetic values calculated by the quadratic element method is always less than those calculated by the linear element method. The improvement of the electric potential is especially important as the distance between the dipole and the measured points decreases; on a realistic head model, the quadratic element method more precisely defines the area of electrical potential. In contrast, the improved quadratic method calculations of magnetic values is increasingly important for detectors remote from the dipole as often is the case in measured MEG. But the quadratic method takes considerably more time than does the linear method for the same RMS accuracy. In calculating the electric and magnetic fields in a realistic head model, the quadratic element method would seem to be best applied to EEG electrodes near the dipole and MEG detectors remote from the dipole. But for EEG electrodes farther away from the dipole and MEG detectors near the dipole, the linear element method could be used as the advantages of the reduced run-time may dominate the minimized error at these distances. This balance between accuracy and computation time may be improved by the use of a model employing an adaptive finite element method.

References

[1] Burnett, D.S. Finite Element Analysis: From Concepts to Applications. Addison-Wesley Publishing Company, 1987.

[2] Jin, J. The Finite Element Method in Electromagnetics. John Wiley & Sons, Inc., 1993.

[3] Klepfer, R.N. Role of Conductivity and Mesh Refinement in Finite Element Computations of Electrocardiographic Fields. PhD thesis, University of Utah, 1999.

[4] Mosher, J.C., Leahy, R.M., and Lewis P.S. EEG and MEG: Forward solutions for inverse methods. IEEE Trans Biomed. Eng., 1999, 46:245-259.

[5] Parker, S.G., Weinstein, D.M., and Johnson, C.R. The SCIRun computational steering software system, In: Arge, E., Bruaset, A.M., and Langtangen, H.P. Modern Software Tools in Scientific Computing, Birkhauser Press, 1997.

[6] Peters, M.J., and De Munck, J.C. The influence of model parameters on the inverse solution based on MEGs and EEGs. Acta Otolaryngol, 1991, 491:61-69.

[7] Pursula, A., Nenonen, J., Somersalo, E., et. al. Bioelectromagnetic calculations in anisotropic volume conductors. Proceedings of Biomag2000, pp. 659-662, Espoo, Finland, August 2000.

[8] Sarvas, J. Basic mathematical and electromagnetic concepts of the biomagnetic inverse problem. Phys. Med. Biol., 1987, 32:11-22.

[9] Strang, G., and Fix, G. An Analysis of the Finite Element Method. Prentice-Hall, 1973.

[10] Yao, D. IEEE Trans. Biomed. Eng., 2000, 47:964-966.

Acknowledgments

This work was supported by NIH NCRR grant 5P41RR012553-02. The authors would like to thank Nathan Galli for his assistance in generating the figures.